INTERNATIONAL JOURNAL OF ROBUST AND NONLINEAR CONTROL
Int. J. Robust Nonlinear Control 2010; **20**:1047–1058
Published online 9 April 2010 in Wiley InterScience (www.interscience.wiley.com). DOI: 10.1002/rnc.1587

Structural adaptation and robustness of *Dictyostelium* ligand–receptor kinetics for low and high ligand concentrations‡

Jongrae Kim[1,2,*,†], Pat Heslop-Harrison[2,3], Ian Postlethwaite[4] and Declan G. Bates[2,5]

[1]*Department of Aerospace Engineering, University of Glasgow, Glasgow G12 8QQ, U.K.*
[2]*Systems Biology Lab (http://www.sblab.org), University of Leicester, Leicester, U.K.*
[3]*Department of Biology, University of Leicester, Leicester, U.K.*
[4]*Northumbria University, Newcastle, U.K.*
[5]*Department of Engineering, University of Leicester, Leicester, U.K.*

SUMMARY

Ligand–receptor interactions are responsible for adaptation and robustness of all cellular life to most chemical external stimuli, and are mediated by cellular networks whose structure appears to be highly conserved among different organisms. Although many ligand–receptor networks exhibit a common structure, the dynamic response to variations in the ligand concentration can be vastly different from network to network. This suggests that certain parameters of the network have evolved by nature to provide appropriate performance and robustness characteristics for different situations. We investigate the system's response in the cases of low and and high concentrations of external cAMP, corresponding to two distinct stages of the *Dictyostelium* life cycle. Our analysis reveals highly robust responses from the ligand-bound receptor kinetics for low ligand concentration, and such high levels of robustness are likely to be required from each individual *Dictyostelium* cell to survive this stage of its life cycle. We show that overshoot is prohibited by the structure of network regardless of the kinetic constants values, and the particular values chosen in the original model are shown to lead to a critically damped response. On the other hand, for high ligand concentrations an extreme reduction in the magnitude of the network response to external signals is observed, and this may be responsible for the completely different physiological behaviour of the organism as groups of up to 10^5 *Dictyostelium* cells aggregate to form a slug. The receptor–ligand interaction networks may have evolved to provide an optimal trade-off between maximizing the speed of response and prohibiting overshoot as it follows external oscillatory signals. Copyright © 2010 John Wiley & Sons, Ltd.

Received 28 March 2009; Revised 4 February 2010; Accepted 5 February 2010

KEY WORDS: *Dictyostelium*; cAMP oscillations; robustness

*Correspondence to: Jongrae Kim, Department of Aerospace Engineering, University of Glasgow, Glasgow G12 8QQ, U.K.
†E-mail: jkim@aero.gla.ac.uk
‡An early version of this paper was presented at the IFAC World Congress, Seoul, Korea, July 6–11, 2008.

Contract/grant sponsor: Biotechnology and Biological Sciences Research Council; contract/grant number: BB/D015340/1

1. INTRODUCTION

In cellular signal transduction, external signalling molecules, called ligands, are initially bound by receptors which are distributed on the cell surface. The ligand–receptor complex then initiates the response of various intracellular signal transduction pathways, such as activation of immune responses, growth factors, etc. Inappropriate activation of signal transduction pathways is considered to be an important factor underlying the development of many diseases. Hence, robust performance of ligand and receptor interaction networks constitutes one of the crucial mechanisms for ensuring the healthy development of living organisms.

In [1], a kinetic model for how the distribution of chemo-receptor complexes affects the cell response was developed from time series responses to perturbations in ligand concentration. By analysing this model, it was identified that the distribution of complex size in the membrane depends on the receptor free energy. Physical details about ligand–receptor interactions are discussed in [2]. In [3], the authors proposed the existence of a generic structure for ligand–receptor interaction networks, and developed a corresponding general model for these types of networks. This model suggests that the ability to capture ligand together with the ability to internalize bound-ligand complexes are the key properties distinguishing the various functional differences in the cell receptor kinetics. The above studies have highlighted the fact that striking structural similarities exist between the various different types of ligand–receptor interaction networks found in nature. It is also tempting to speculate that nature would have evolved the parameters in such structural networks to deliver robust and optimal (for each particular situation) performance in relaying external signals into the cell [4–8]. In this paper, we show how analysis tools from control engineering may be used to provide a specific example of a cellular system which seems to support both of the above hypotheses.

Dictyostelium discoideum are social amoebae which have been widely used as model organisms for studying key processes in molecular biology [9]. Under normal conditions, *Dictyostelium* cells grow independently by feeding on bacteria in forest soil, but under conditions of starvation they initiate a well-defined program of development [10]. In this program, the individual cells aggregate by sensing and moving towards gradients in cAMP (cyclic Adenosine Mono-Phosphate), a process known as chemotaxis, to form complexes of up to 10^5-cells. Subsequently, the individual cells form a slug which eventually becomes a fruiting body which emits spores. The early stages of aggregation are initiated by the production of spontaneous oscillations in the concentration of cAMP (and several other molecular species) inside the cell. While the cells are aggregating, they show remarkable sensitivity to small changes in external cAMP concentrations, with only a difference of a few molecules being sufficient to make the cell move correctly towards the region of higher concentration. On the other hand, as *Dictyostelium* cells approach close to each other and form a slug, cell-to-cell adhesion and surface contacts also contribute important effects [11].

In [10, 12] a model, consisting of a set of nonlinear ordinary differential equations, was developed to explain the processes underlying the spontaneous oscillations that occur in the early stages of *Dictyostelium* aggregation. Note that the oscillations for each individual cell are not completely autonomous, but are excited by changes in the concentration of external cAMP, which is secreted from each cell and diffuses throughout the region where the cells are distributed. Thus, for this system, external cAMP molecules constitute the ligand, while molecules on the surface of the *Dictyostelium* cells called CAR1 (Catabolism of ARginine) constitute the receptors.

In this paper, we show that the above ligand–receptor interaction network exhibits the generic network structure postulated in [3]. The dynamics of the *Dictyostelium* cAMP network for both low and high external cAMP concentrations are compared with the responses of the epidermal growth factor receptor (EGFR) network, which is related to development and tumorigenesis, the transferrin receptor (TfR) network, which enables iron uptake from the extracellular space, and the vitellogenin receptor (VtgR) network, which is a transport receptor used during oogenesis in many oviparous species [3].

DOI: 10.1002/rnc

2. A GENERIC STRUCTURE FOR LIGAND–RECEPTOR INTERACTION NETWORKS

A generic structure for cellular ligand–receptor interaction networks of the following form is proposed in [3]:

$$L+R \underset{k_{\text{off}}}{\overset{k_{\text{on}}}{\rightleftharpoons}} C, \quad Q_R \xrightarrow{1} R, \quad f(t) \xrightarrow{1} L, \quad R \xrightarrow{k_t} \emptyset, \quad C \xrightarrow{k_e} \emptyset, \tag{1}$$

where L is the ligand concentration, R is the number of external cell receptor molecules, C is the number of ligand–receptor complex molecules, k_{on} is the forward reaction rate for ligands binding to receptors, k_{off} is the reverse reaction rate for ligands dissociating from receptors, k_t is the rate of internalization of receptor molecules, k_e is the rate of internalization of ligand–receptor complexes, and Q_R is equal to $R_T \times k_t$. R_T is the steady-state number of cell surface receptors when $C=0$ and $L=0$, $\emptyset$ represents the sinks of either the receptor or the complex, $f(t)$ is an external stimulus signal and t is time. The corresponding differential equations are given by

$$\frac{\mathrm{d}}{\mathrm{d}t}\begin{bmatrix} R \\ C \\ L \end{bmatrix} = \begin{bmatrix} -k_{\text{on}}RL + k_{\text{off}}C - k_t R + Q_R \\ k_{\text{on}}RL - k_{\text{off}}C - k_e C \\ -\dfrac{k_{\text{on}}}{N_{\text{av}}V_{\text{c}}}RL + \dfrac{k_{\text{off}}}{N_{\text{av}}V_{\text{c}}}C + f(t) \end{bmatrix}, \tag{2}$$

where N_{av} is Avogadro's number, 6.023×10^{23} and V_{c} is the cell volume in liters throughout which the receptors are distributed.

In normalized form, the above equation can be written as

$$\frac{\mathrm{d}}{\mathrm{d}t^*}\begin{bmatrix} R^* \\ C^* \\ L^* \end{bmatrix} = \begin{bmatrix} -R^*L^* + C^* - \alpha(R^*-1) \\ R^*L^* - C^* - \beta C^* \\ -\gamma R^*L^* + \gamma C^* + u(t) \end{bmatrix}, \tag{3}$$

where $t^* = k_{\text{off}}t$, $R^* = R/R_T$, $C^* = C/R_T$, $L^* = L/K_{\text{D}}$, $u(t) = f(t)/(k_{\text{off}}K_{\text{D}})$ K_{D} is the receptor dissociation constant, i.e. $K_{\text{D}} = k_{\text{off}}/k_{\text{on}}$, $\alpha = k_t/k_{\text{off}}$, $\beta = k_e/k_{\text{off}}$, $\gamma = K_a R_T/(N_{\text{av}}V_{\text{c}})$, and $K_a = 1/K_{\text{D}}$. α is a quantity proportional to the probability of internalization of unbound receptors, β is a quantity proportional to the probability of internalization of captured ligand by receptors before dissociation of the ligand from the receptors, and γ represents the level of sensitivity of the receptors to the external signals [3].

The above kinetics can be simplified for two extreme cases, i.e. low and high ligand concentrations. These two cases are of particular interests for various biomolecular networks and they demonstrate different optimality and robustness properties of the ligand–receptor kinetics. By assuming that the number of receptors is much larger than the number of ligands, i.e. $\mathrm{d}R/\mathrm{d}t \approx 0$ ($R \approx R_T$), which is the case for low ligand concentrations, the following approximations for the ligand/complex and ligand kinetics are obtained:

$$\frac{\mathrm{d}}{\mathrm{d}t^*}\begin{bmatrix} C^* \\ L^* \end{bmatrix} = \begin{bmatrix} -(1+\beta) & 1 \\ \gamma & -\gamma \end{bmatrix}\begin{bmatrix} C^* \\ L^* \end{bmatrix} + \begin{bmatrix} 0 \\ 1 \end{bmatrix} u(t). \tag{4}$$

On the other hand, by assuming that the number of ligands is much larger than the number of receptors, i.e. $\mathrm{d}L/\mathrm{d}t \approx 0$ ($L \approx$ constant), which is the case for high ligand concentrations, the following approximations for the

DOI: 10.1002/rnc

ligand/complex and receptor kinetics are obtained:

$$\frac{\mathrm{d}}{\mathrm{d}t^*}\begin{bmatrix} C^* \\ R^* \end{bmatrix} = \begin{bmatrix} -(1+\beta) & L^* \\ 1 & -(L^*+\alpha) \end{bmatrix}\begin{bmatrix} C^* \\ R^* \end{bmatrix} + \begin{bmatrix} 0 \\ 1 \end{bmatrix}\alpha, \tag{5}$$

where L^* remains approximately constant and is equal to L/K_{D}.

3. LIGAND–RECEPTOR INTERACTION NETWORK OF AGGREGATING *DICTYOSTELIUM* CELLS

We now show in Figure 1 how a ligand–receptor interaction network displaying the generic structure given in the previous section may be extracted in a straightforward manner from a model for the network underlying cAMP oscillations in *Dictyostelium* published in [10, 12] and extended for synchronizing mechanism in [13]. In the figure, arrows show activation, broken arrows show degradation, and the bar arrows represent inhibition.

The corresponding model consists of a set of nonlinear differential equations in the following form:

$$\frac{\mathrm{d}[\mathrm{ACA}]}{\mathrm{d}t} = k_1[\mathrm{CAR1}] - k_2[\mathrm{ACA}][\mathrm{PKA}],$$

$$\frac{\mathrm{d}[\mathrm{PKA}]}{\mathrm{d}t} = k_3[\mathrm{cAMPi}] - k_4[\mathrm{PKA}],$$

$$\frac{\mathrm{d}[\mathrm{ERK2}]}{\mathrm{d}t} = k_5[\mathrm{CAR1}] - k_6[\mathrm{PKA}][\mathrm{ERK2}],$$

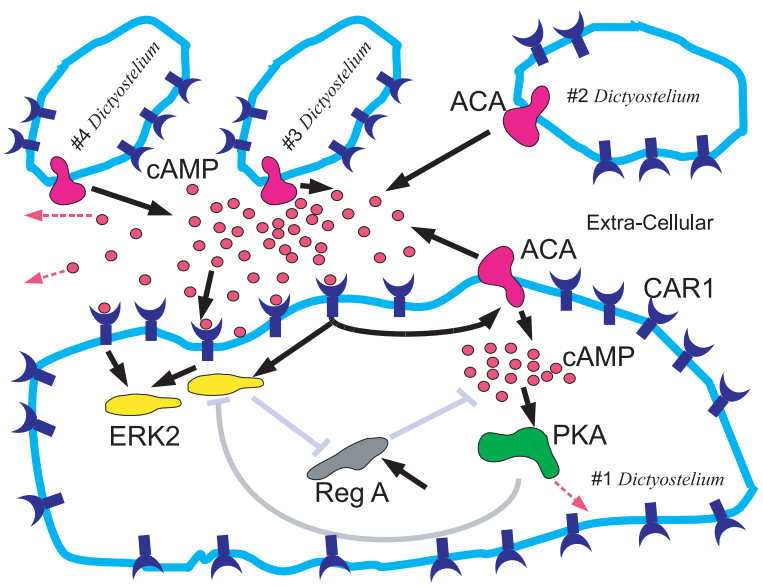

Figure 1. *Dictyostelium* cAMP oscillation network, where the figures are not to scale and the details for #2, #3 and #4 *Dictyostelium*'s are omitted.

DOI: 10.1002/rnc

$$\begin{aligned}
\frac{\mathrm{d}[\mathrm{RegA}]}{\mathrm{d}t} &= k_7 - k_8[\mathrm{ERK2}][\mathrm{RegA}], \\
\frac{\mathrm{d}[\mathrm{cAMPi}]}{\mathrm{d}t} &= k_9[\mathrm{ACA}] - k_{10}[\mathrm{RegA}][\mathrm{cAMPi}], \\
\frac{\mathrm{d}[\mathrm{cAMPe}]}{\mathrm{d}t} &= k_{11}[\mathrm{ACA}] - k_{12}[\mathrm{cAMPe}] + \sum_{i=2}^{n} \tilde{k}_{11}^{i}[\mathrm{ACA}_i], \\
\frac{\mathrm{d}[\mathrm{CAR1}]}{\mathrm{d}t} &= k_{13}[\mathrm{cAMPe}] - k_{14}[\mathrm{CAR1}],
\end{aligned} \tag{6}$$

where ACA is adenylyl cyclase, PKA is the protein kinase, ERK2 is the mitogen-activated protein kinase, RegA is the cAMP phosphodiesterase, and cAMPi and cAMPe are the internal and the external cAMP concentrations, respectively. CAR1 stands for the ligand-bound cell receptor, but in the above equation it indicates the ligand–receptor complex. $\sum \tilde{k}_{11}^{i}[\mathrm{ACA}_i]$ is the contribution to the external cAMP from the other *Dictyostelium*, where the diffusion effect is negligible as the distance between cells are assumed to be close enough, n is the number of cells, and $\tilde{k}_{11}^{i}$ is the external cAMP secretion rate for the ith *Dictyostelium*, which is not necessarily the same value as the ones for the other *Dictyostelium*.

In the next two sections, the biologically important cases of low and high ligand concentrations are considered. From now on, L and C correspond to cAMPe and CAR1 in (6), respectively, and the same notation R is used for the CAR1 receptor.

3.1. Low ligand concentration

Consider first the low ligand concentration case. The ligand–receptor interaction network for this case can be extracted from (6) as follows:

$$\frac{\mathrm{d}}{\mathrm{d}t}\begin{bmatrix}[\mathrm{CAR1}\\ [\mathrm{cAMPe}]\end{bmatrix} = \begin{bmatrix}-k_{14} & k_{13}\\ 0 & -k_{12}\end{bmatrix}\begin{bmatrix}[\mathrm{CAR1}(t)]\\ [\mathrm{cAMPe}(t)]\end{bmatrix} + \begin{bmatrix}0\\ k_{11}\end{bmatrix}[\mathrm{ACA}(t)] + \sum_{i=2}^{n}\begin{bmatrix}0\\ \tilde{k}_{11}^{i}\end{bmatrix}[\mathrm{ACA}_i(t)]. \tag{7}$$

More than 10 cells are locally synchronized in the aggregation phase [14], the effect of [ACA] could be ignored as comparing with the ones from the other cells as follows:

$$\frac{\mathrm{d}}{\mathrm{d}t}\begin{bmatrix}[\mathrm{CAR1}\\ [\mathrm{cAMPe}]\end{bmatrix} \approx \begin{bmatrix}-k_{14} & k_{13}\\ 0 & -k_{12}\end{bmatrix}\begin{bmatrix}[\mathrm{CAR1}(t)]\\ [\mathrm{cAMPe}(t)]\end{bmatrix} + \sum_{i=2}^{n}\begin{bmatrix}0\\ \tilde{k}_{11}^{i}\end{bmatrix}[\mathrm{ACA}_i(t)]. \tag{8}$$

Note that in the above, $[\mathrm{CAR1}(t)]$, $[\mathrm{cAMPe}(t)]$, $[\mathrm{ACA}(t)]$, and $[\mathrm{ACA}_i(t)]$ are concentrations in units of μM and k_{11}, $\tilde{k}_{11}$, k_{12}, k_{13}, and k_{14} are reaction constants in units of 1/min. To transform the unit of $\mathrm{CAR1}(t)$ into the number of molecules, we use the relation, $C = [\mathrm{CAR1}(t)]N_{\mathrm{av}}V_{\mathrm{c}}$, and hence derive the following:

$$\frac{\mathrm{d}C}{\mathrm{d}t} = -k_{14}[\mathrm{CAR1}(t)]N_{\mathrm{av}}V_{\mathrm{c}} + k_{13}[\mathrm{cAMPe}(t)]N_{\mathrm{av}}V_{\mathrm{c}} = -k_{14}C + k_{13}N_{\mathrm{av}}V_{\mathrm{c}}L, \tag{9}$$

where $L = [\mathrm{cAMPe}(t)]$. In addition,

$$\frac{\mathrm{d}L}{\mathrm{d}t} = -k_{12}L + \sum_{i=2}^{n}\tilde{k}_{11}^{i}[\mathrm{ACA}_i(t)]. \tag{10}$$

DOI: 10.1002/rnc

With the normalized states,

$$\frac{dC^*}{dt^*} = -\frac{k_{14}}{k_{off}} C^* + \frac{k_{13} N_{av} V_c}{R_T k_{on}} L^*. \tag{11}$$

Then,

$$\frac{dC^*}{dt^*} = -\frac{k_{14}}{k_{off}} C^* + L^{**}, \tag{12}$$

where $L_L^{**} = L^* K_L$ and $K_L = (k_{13} N_{av} V_c)/(R_T k_{on})$. Note that K_L is multiplied by L^* to make the coefficient equal to one as in (4). Similarly,

$$\frac{dL_L^{**}}{dt^*} = -\frac{k_{12}}{k_{off}} L_L^{**} + u, \tag{13}$$

where

$$u = \frac{K_L}{K_D k_{off}} \sum_{i=2}^{n} \tilde{k}_{11}^i [\mathrm{ACA}_i(t)]. \tag{14}$$

In a compact form,

$$\frac{d}{dt} \begin{bmatrix} C^* \\ L_L^{**} \end{bmatrix} = \begin{bmatrix} -k_{14}/k_{off} & 1 \\ 0 & -k_{12}/k_{off} \end{bmatrix} \begin{bmatrix} C^* \\ L_L^{**} \end{bmatrix} + \begin{bmatrix} 0 \\ 1 \end{bmatrix} u. \tag{15}$$

Comparing (15) with (4), we notice that there are some differences in the structures of the two equations. However, this is mainly because of the effect of the $k_{off}C$ term in (2). Including only the external response part, (4) can be rewritten as follows:

$$\frac{d}{dt^*} \begin{bmatrix} C^* \\ L_L^{**} \end{bmatrix} = \begin{bmatrix} -\beta & 1 \\ 0 & -\gamma \end{bmatrix} \begin{bmatrix} C^* \\ L_L^{**} \end{bmatrix} + \begin{bmatrix} 0 \\ 1 \end{bmatrix} u. \tag{16}$$

Then, the following relations are obtained:

$$\beta = \frac{k_{14}}{k_{off}}, \quad \gamma = \frac{k_{12}}{k_{off}}. \tag{17}$$

Although the generic ligand–receptor interaction network structure certainly seems to be used in this model of how *Dictyostelium* cells generate cAMP oscillations, it can be immediately seen that a profound difference also exists. Unlike (12), the effect of C^* to dL_L^{**}/dt^* is zero. Thus, the rate of dissociation of the ligand from the receptor is very low, i.e. once the cAMP ligand is caught by the CAR1 receptors, it is rarely released before being absorbed into the cell.

The values of the constants in the above equations are given as follows: $k_{11} = 0.7\,\mathrm{min}^{-1}$, $k_{12} = 4.9\,\mathrm{min}^{-1}$, $k_{13} = 23.0\,\mathrm{min}^{-1}$, $k_{14} = 4.5\,\mathrm{min}^{-1}$, $R_T = 4 \times 10^4$, [12, 15], and $k_{off} = 0.7 \times 60\,\mathrm{min}^{-1}$, and $k_{on} = 0.7 \times 60 \times 10^7\,\mathrm{M}^{-1}\,\mathrm{min}^{-1}$ [16]. Hence, $\beta = 0.107$ and $\gamma = 0.117$. In [17], the average diameter and volume of a *Dictyostelium* cell are given to be $10.25\,\mu\mathrm{m}$ and $565\,\mu\mathrm{m}^3$. To calculate V_c, we consider an approximation for the shape of a *Dictyostelium* cell as a cylinder. Since the cell receptors are only distributed on the surface of the cell, the interior of the cell must be extracted to calculate an effective volume that represents the space where all molecular interactions occur under well-mixed conditions. The effective volume is determined such that the maximum number of ligand-bound CAR1 molecules is about 1% of the total number of receptors, to give a value of V_c equal to 1.66×10^{-16} l. These values were verified using a stochastic simulation of the Laub–Loomis model with Gillespie's direct method [18].

DOI: 10.1002/rnc

3.2. High ligand concentration

Similarly, the ligand–receptor interaction network for high ligand concentrations can be extracted from (6) as follows:

$$\frac{\mathrm{d}}{\mathrm{d}t}\begin{bmatrix} C \\ R \end{bmatrix} = \begin{bmatrix} -k_{14}C + k_{13}N_{\mathrm{av}}V_{\mathrm{c}}[\mathrm{cAMPe}(t)] \\ -k_{13}N_{\mathrm{av}}V_{\mathrm{c}}[\mathrm{cAMPe}(t)] - k_t R + Q_R \end{bmatrix}, \tag{18}$$

where k_{13} corresponds to the rate of ligand–receptor complex generation where the number of receptors is constant. Therefore, in this case the number of unoccupied receptors is changing significantly and thus $k_{13}N_{\mathrm{av}}V_{\mathrm{c}}$ is replaced by $k_{\mathrm{on}}R$. Hence,

$$\frac{\mathrm{d}}{\mathrm{d}t}\begin{bmatrix} C \\ R \end{bmatrix} = \begin{bmatrix} -k_{14} & k_{\mathrm{on}}L \\ 0 & -k_{\mathrm{on}}L - k_t \end{bmatrix}\begin{bmatrix} C \\ R \end{bmatrix} + \begin{bmatrix} 0 \\ 1 \end{bmatrix} Q_R, \tag{19}$$

where for this case of high ligand concentrations the concentration of cAMPe, i.e. L, is considered as a constant, C and R are in units of the number of molecules, and L is in units of M (molar). The ligand–receptor complex is assumed to be completely internalized as in the low ligand concentration case. Normalizing in the same way as for the previous case, the following equations are obtained:

$$\frac{\mathrm{d}}{\mathrm{d}t^*}\begin{bmatrix} C^* \\ R^* \end{bmatrix} = \begin{bmatrix} -\beta & L_a^{**} \\ 0 & -(L_a^{**} + \alpha) \end{bmatrix}\begin{bmatrix} C^* \\ R^* \end{bmatrix} + \begin{bmatrix} 0 \\ 1 \end{bmatrix} \alpha, \tag{20}$$

where $L_a^{**} = K_a L$. Again, the rate of dissociation of the ligand from the receptor is assumed to be very low and the effect of C^* to $\mathrm{d}R^*/\mathrm{d}t^*$ is zero.

4. DYNAMIC CHARACTERISTICS OF THE *DICTYOSTELIUM* LIGAND–RECEPTOR INTERACTION NETWORK

In this section we analyse the optimality and robustness of the parameters in the *Dictyostelium* ligand–receptor interaction network for low and high ligand concentrations.

4.1. Low ligand concentration

For the low ligand concentration case, differentiating both sides of 12 with respect to the normalized time, t^*, we get

$$\frac{\mathrm{d}^2C^*}{\mathrm{d}t^{*2}} = \frac{-k_{14}}{k_{\mathrm{off}}}\frac{\mathrm{d}C^*}{\mathrm{d}t^*} + \frac{\mathrm{d}L^{**}}{\mathrm{d}t^*} = \frac{-k_{14}}{k_{\mathrm{off}}}\frac{\mathrm{d}C^*}{\mathrm{d}t^*} - \frac{k_{12}}{k_{\mathrm{off}}}\left(\frac{\mathrm{d}C^*}{\mathrm{d}t^*} + \frac{k_{14}}{k_{\mathrm{off}}}C^*\right) + u. \tag{21}$$

Hence, the ligand–receptor complex kinetics for the low ligand concentration case are given by

$$\ddot{C}^* + \frac{k_{12}+k_{14}}{k_{\mathrm{off}}}\dot{C}^* + \frac{k_{12}k_{14}}{k_{\mathrm{off}}^2}C^* = u, \tag{22}$$

where the single and the double dot represent $d(\cdot)/\mathrm{d}t^*$ and $d^2(\cdot)/\mathrm{d}t^{*2}$, respectively.

Since (22) is simply a second-order linear ordinary differential equations, we can define the natural frequency, ω_n, and the damping ratio, ζ as follows:

$$\ddot{C}^* + 2\zeta\omega_n\dot{C}^* + \omega_n^2 C^* = u. \tag{23}$$

DOI: 10.1002/rnc

Comparing (22) with (23) we have that

$$\omega_n = \frac{\sqrt{k_{12}k_{14}}}{k_{\text{off}}}, \quad \zeta = \frac{k_{12}+k_{14}}{2\sqrt{k_{12}k_{14}}}. \tag{24}$$

Substituting the appropriate values for the *Dictyostelium* network, we find that ω_n is equal to 0.112 and ζ is equal to 1.001. The overshoot, M_p, and the settling time, t_s, for a step input are given by [19]

$$M_p = \begin{cases} e^{-\pi\zeta/\sqrt{1-\zeta^2}} & \text{for } 0 \leqslant \zeta < 1, \\ 0 & \text{for } \zeta \geqslant 1, \end{cases} \tag{25a}$$

$$t_s = \frac{-\ln 0.01}{\zeta\omega_n}. \tag{25b}$$

Thus, the kinetics of the *Dictyostelium* ligand–receptor network produce a system with a damping ratio almost exactly equal to 1, i.e. the critical damping ratio. The critical damping ratio is the optimal solution for maximizing the speed of a system's response without allowing any overshoot:

$$\zeta^* = \arg\min t_s(\zeta) \tag{26}$$

subject to $M_p = 0$ and (22). It appears that *Dictyostelium* cells may have evolved a receptor–ligand interaction network which provides an optimal trade-off between maximizing the speed of response and prohibiting overshoot so that it can follow oscillatory external signals with a certain frequency.

In Table I, the values of the network parameters for three other ligand–receptor networks (discussed in [3]) are shown. As it is clear from the values of the damping ratio of *Dictyostelium* for low and high ligand concentration cases (Table II), the responses are over-damped and thus no overshoot to fast changes in ligand concentrations will occur. Indeed, in the case of the *Dictyostelium* network, the possibility of overshoot is completely prohibited, since the damping ratio cannot be less than one for any combination of the kinetic parameters. This can be seen by considering the fact that

$$\zeta = \frac{k_{12}+k_{14}}{2\sqrt{k_{12}k_{14}}} \geqslant 1 \Leftrightarrow (k_{12}-k_{14})^2 \geqslant 0 \tag{27}$$

for all $k_{12} > 0$ and $k_{14} > 0$. Hence, the over-damped nature of the dynamical response stems from the network structure itself, rather than being dependent on any particular value of the kinetic parameters. For this level of uncertainty in the kinetic parameters, the settling times vary between 35 and 105 min (for the nominal parameter values, the settling time is about 52 min). Each step response for various perturbation combinations is shown in Figure 2, where each kinetic parameter is perturbed by up to $\pm 50\%$ and the response is normalized by the value of each steady state.

Table I. Kinetic parameters for EGFR, TfR and VtgR ligand–receptor networks [3].

	k_e	k_t	k_{off}	K_{D} [nM]	R_T	V_{c}
EGFR	0.15	0.02	0.24	2.47	2×10^{5}	4×10^{-10}
TfR	0.6	0.6	0.09	29.8	2.6×10^{4}	4×10^{-10}
VtgR	0.108	0.108	0.07	1300	2×10^{11}	4×10^{-10}

DOI: 10.1002/rnc

Table II. Damping ratio (ζ) and natural frequency (ω_n) for low and high ligand concentration.

	$L \ll 1\,\mu M$		$L = 10\,\mu M$	
	ζ	ω_n	ζ	ω_n
EGFR	1.40	0.58	0.18	20.12
TfR	63.70	0.06	1.59	5.79
VtgR	0.05	25.27	1.36	0.88
Dictyostelium	1.00	0.11	15.3	3.27

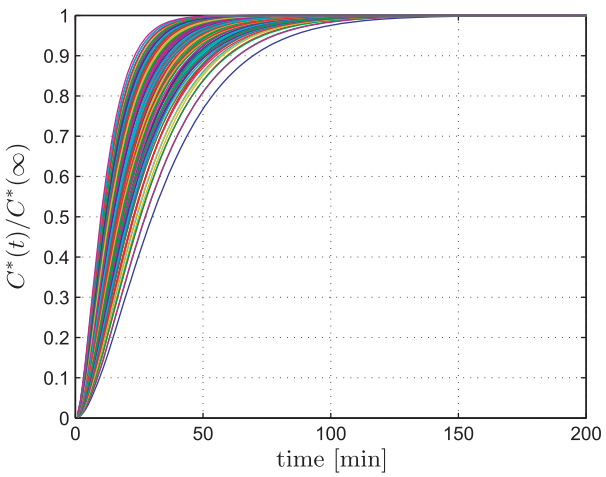

Figure 2. Step responses with the perturbed parameters k_{12} and k_{14}.

One significant difference between the *Dictyostelium* network and the other ligand–receptor networks shown in Table I is its relatively fast response time. Since aggregating *Dictyostelium* cells exhibit oscillatory behaviour, rather than converging to a constant steady state, the ligand–receptor interaction network may have evolved to maximize the speed of response, in order to ensure the generation of robust and stable limit cycles for low concentrations of external cAMP. This can be more clearly seen in the Bode plots for the responses of the different networks, which are shown in Figure 3(a).

The region inside the two dashed vertical lines corresponds to oscillations with periods between 5 and 10 min, which is the range of cAMP oscillations observed experimentally in the early stages of aggregation of *Dictyostelium*. The bandwidth of the *Dictyostelium* ligand–receptor kinetics is about 3 rad/min, which is just above the minimum necessary to facilitate the oscillations in cAMP with a period of 5–10 min observed in *Dictyostelium* during chemotaxis.

Recall that from the definition of $u(t)$,

$$u = \frac{K_L}{K_D k_{off}} \sum_{i=2}^{n} \tilde{k}_{11}^{i} [ACA_i(t)] = \frac{k_{13} N_{av}}{k_{off}^2} \frac{V_c}{R_T} \sum_{i=2}^{n} \tilde{k}_{11}^{i} [ACA_i(t)] \tag{28}$$

the cell volume, V_c, and the total number of receptors, R_T, appear only in the definition of u in (22). Hence, variations in V_c and R_T can affect the static gain of the response but they have no effect on its dynamic characteristics. Moreover, it is most likely that the total number of receptors increases as the cell volume increases, i.e, $V_c/R_T \approx$ (constant).

DOI: 10.1002/rnc

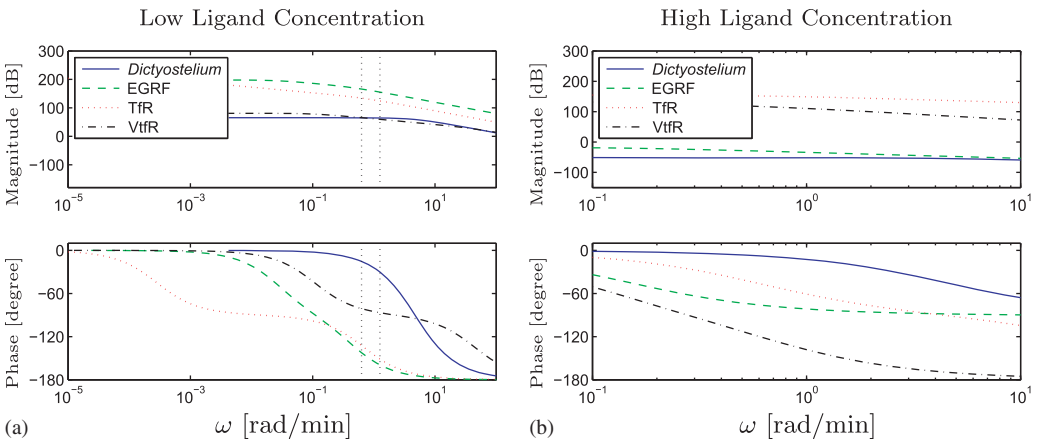

Figure 3. Bode plots for low/high ligand concentrations.

Under this assumption, even the static gain will be relatively insensitive to variations in the cell volume and in the number of receptors. Therefore, the maximum peak (M_p) of the network's impulse responses should be very robust with respect to variations in the cell volume (V_c) and in the number of cell receptors (R_T).

4.2. High ligand concentration

Similarly, for the high ligand concentration case, the following is obtained:

$$\ddot{C}^* + \frac{k_t + k_{on}L + k_{14}}{k_{off}}\dot{C}^* + \frac{(k_t + k_{on}L)k_{14}}{k_{off}^2}C^* = L_a^{**}\alpha. \tag{29}$$

Again, comparing (29) with (23), the natural frequency and the damping factor are given by

$$\omega_n = \frac{\sqrt{(k_t + k_{on}L)k_{14}}}{k_{off}}, \quad \zeta = \frac{k_t + k_{on}L + k_{14}}{2\sqrt{(k_t + k_{on}L)k_{14}}}, \tag{30}$$

where L is assumed to be equal to 10 μM, which is about a 20 times higher concentration than that produced in normal cAMP oscillations during the early stages of *Dictyostelium* chemotaxis. Substituting the values for the *Dictyostelium* network, we find that ω_n is equal to 3.27 and ζ is equal to 15.3. As noted in [20], k_t could vary within a 20 times range from the minimum to the maximum, i.e. between 0.012 and 0.22 min^{-1}. However, the value of k_t is significantly smaller than $k_{on}L$ or k_{14} and thus the effects of k_t in the natural frequency and the damping factor are negligible . Hence, the ligand–receptor complex kinetics for the high ligand concentration case are approximated by

$$\ddot{C}^* + \frac{k_{on}L + k_{14}}{k_{off}}\dot{C}^* + \frac{(k_{on}L)k_{14}}{k_{off}^2}C^* = L_a^{**}\alpha. \tag{31}$$

Therefore, the dynamics of the network will be highly robust to variations in the receptor internalization rate, since variations in k_t only affect the size of the input, i.e. α, and, considering the high ligand concentration, even this effect is likely to be minor. In addition, similar to the low ligand case the under-damping is prohibited for the high ligand concentration case as well (Table II).

DOI: 10.1002/rnc

The Bode plots for the high ligand concentration case are shown in Figure 3(b). The *Dictyostelium* and EGFR networks show the most significant changes in their frequency responses for the two extreme ligand concentration cases. Based on the values of β and γ derived for the *Dictyostelium* and EGFR networks, both may be categorized as dual-sensitivity networks, i.e. these networks achieve an optimal balance between maximizing the probability to capture external signals and maximizing the probability to internalize the captured signal—see [3] for a full discussion. Finally, as shown in [12], the peak activity of ERK2 during spontaneous cAMP oscillation is when external cAMP concentration is a very low concentration, around 1 nM. Therefore, the response to high cAMP concentrations would naturally be reduced as characterized in Figure 3. These extreme sensitivity changes in the response of *Dictyostelium* to different external cAMP concentrations may be responsible for the completely different behaviours exhibited by individual *Dictyostelium* cells and the *Dictyostelium* slug formed at the end of the aggregation process.

5. CONCLUSIONS

Correct functioning of ligand–receptor interactions is crucial to the survival of organisms, and these interactions are mediated by cellular networks whose structure appears to be highly conserved in nature. However, the wide variation in the dynamic responses of different ligand–receptor networks suggests that certain parameters of the network are optimized by evolution to provide appropriate performance and robustness characteristics for particular situations. In this paper, we showed how analysis tools from Control Engineering could be used to study the dynamical characteristics of the ligand–receptor network involved in generating cAMP oscillation in aggregating *Dictyostelium* cells. Using a recently proposed generic model for ligand–receptor networks, we investigated the system's response in the cases of low and and high concentrations of external cAMP, corresponding to two distinct stages of the *Dictyostelium* life cycle. Our analysis revealed highly robust responses for the ligand–bound receptor kinetics for low ligand concentration, and indeed such high levels of robustness are likely to be required from each individual cell in order to survive this stage of its life cycle. *Dictyostelium* cells may have evolved a receptor–ligand interaction network which maximizes the speed of response for the given structure that prohibits any overshoot of the response to external signals. On the other hand, for high ligand concentrations an extreme reduction in the magnitude of the network response to external signals is observed. We postulate that this may be responsible for the completely different physiological behaviour of the organism as groups of up to 10^5 *Dictyostelium* cells aggregate to form a slug.

ACKNOWLEDGEMENTS

This work was supported by BBSRC research grant BB/D015340/1.

REFERENCES

1. Eendre RG, Falke JJ, Wingreen NS. Chemotaxis receptor complexes: from signaling to assembly. *PLoS Computational Biology* 2007; **3**(7). DOI: 10.1371/journal.pcbi.0030150.
2. Bongrand P. Ligand–receptor interactions. *Reports on Progress in Physics* 1999; **62**(6):921–968.
3. Shankaran H, Resat H, Wiley HS. Cell surface receptors for signal transduction and ligand transport: a design principles study. *PLoS Computational Biology* 2007; **3**(6). DOI: 10.1371/journal.pcbi.0030101.
4. Barkai N, Leibler S. Robustness in simple biochemical networks. *Nature* 1999; **387**(26):913–917.
5. Csete ME, Doyle JC. Reverse engineering of biological complexity. *Science* 2002; **295**(5560):1664–1669.
6. Morohashi M, Winnz AE, Borisuk MT, Bolouri H, Doyle JC, Kitano H. Robustness as a measure of plausibility in models of biochemical networks. *Journal of Theoretical Biology* 2002; **216**(1):19–30.

7. Kurata H, El-Samad H, Iwasaki R, Ohtake H, Doyle JC, Grigorova I, Gross CA, Khammash M. Module-based analysis of robustness tradeoffs in the heat shock response system. *PLoS Computational Biology* 2006; **2**(7). DOI: 10.1371/journal.pcbi.0020059.
8. Ciliberti S, Martin OC, Wagner A. Robustness can evolve gradually in complex regulatory gene networks with varying topology. *PLoS Computational Biology* 2007; **3**(2). DOI: 10.1371/journal.pcbi.0030015.
9. Kim J, Bates DG, Postlethwaite I, Ma L, Iglesias PA. Robustness analysis of biochemical network models. *IEE Proceeding Systems Biology* 2006; **153**(3):96–104.
10. Laub MT, Loomis WF. A molecular network that produces spontaneous oscillations in excitable cells of *Dictyostelium*. *Molecular Biology of the Cell* 1998; **9**(12):3521–3532.
11. Weijer CJ. *Dictyostelium* morphogenesis. *Current Opinion in Genetics and Development* 2004; **14**(4):392–398.
12. Maeda M, Lu S, Shaulsky G, Miyazaki Y, Kuwayama H, Tanaka Y, Kuspa A, Loomis WF. Periodic signaling controlled by an oscillatory circuit that includes protein kinases ERK2 and PKA. *Science* 2004; **304**(5672):875–878.
13. Kim J, Heslop-Harrison P, Postlethwaite I, Bates DG. Stochastic noise and synchronization during *Dictyostelium* aggregation make cAMP oscillations robust. *PLoS Computational Biology* 2007; **3**(11). DOI: 10.1371/journal.pcbi.0030218.
14. Lauzeral J, Halloy J, Goldbeter A. Desynchronization of cells on the developmental path triggers the formation of spiral waves of cAMP during *Dictyostelium* aggregation. *Proceedings of the National Academy of Sciences* 1997; **94**(17):9153–9158.
15. Bankir L, Ahloulay M, Devreotes PN, Parent CA. Extracellular cAMP inhibits proximal reabsorptionsalik are plasma membrane cAMP receptors involved. *American Journal of Physiology. Renal Physiology* 2002; **282**(3):376–392.
16. Ishii D, Ishikawa KL, Fujita T, Nakazawa M. Stochastic modelling for gradient sensing by chemotactic cells. *Science and Technology of Advanced Materials* 2004; **5**(5–6):715–718.
17. Soll DR, Yarger J, Mirick M. Stationary phase and the cell cycle of *Dictyostelium discoideum* in liquid nutrient medium. *Journal of Cell Science* 1976; **20**(3):513–523.
18. Gillespie DT. Exact stochastic simulation of coupled chemical reactions. *The Journal of Physical Chemistry* 1977; **81**(25):2340–2361.
19. Franklin GF, Powell JD, Emani-Naeini A. *Feedback Control of Dynamic Systems* (3rd edn). Addison-Wesley: Reading, MA, 1994.
20. Devreotes PN, Sherring JA. Kinetics and concentration dependence of reversible cAMP-induced modification of the surface cAMP receptor in Dictyostelium. *Journal of Biological Chemistry* 1985; **260**(10):6378–6384.